IEEE Access
Multidisciplinary | Rapid Review | Open Access Journal

Received November 8, 2018, accepted November 21, 2018, date of publication November 27, 2018,
date of current version December 27, 2018.

Digital Object Identifier 10.1109/ACCESS.2018.2883435

A Novel Single-Beacon Navigation Method for Group AUVs Based on SIMO Model

SIBO SUN[1,2,3], SHUANGNING YU[2,4], ZHIBO SHI[2,4], JIN FU[1,2], AND CHUNHUI ZHAO[3]

[1]Acoustic Science and Technology Laboratory, Harbin Engineering University, Harbin 150001, China
[2]College of Underwater Acoustic Engineering, Harbin Engineering University, Harbin 150001, China
[3]College of Information and Communication Engineering, Harbin Engineering University, Harbin 150001, China
[4]Key Laboratory of Marine Information Acquisition and Security (Harbin Engineering University), Ministry of Industry and Information Technology, Harbin 150001, China

Corresponding author: Jin Fu (fujin@hrbeu.edu.cn)

This work was supported in part by the National Key R&D Plan under Grant 2017YFC0306900, in part by the National Natural Science Foundation of China under Grant G61801138, in part by the Basic Technical Research Project under Grant JSJL2016604B003, and in part by the China Postdoctoral Science Foundation under Grant 2018M631910.

ABSTRACT Single-beacon navigation for group autonomous underwater vehicles (AUVs) suffers from long navigation period and asynchronization. This paper addresses the problem by introducing the single-input-multiple-output (SIMO) model, where, a single AUV transmits the signal and other AUVs receive the signal. Utilizing the time-delay of signals from the beacon and the sender, the navigation for all AUVs is achieved simultaneously, and the navigation period is dramatically decreased. Moreover, based on the new SIMO model, a tracking method utilizing extended Kalman filter is also put forward to increase the navigation precision and reduce the computational burden. Finally, a coordinate fusion algorithm based on the location, error, and time-delay is presented, which fuses the independent AUV coordinates to be a higher precision holistic coordinate system for group AUVs. Simulation results show the effectiveness of the proposed method.

INDEX TERMS Underwater, navigation, autonomous underwater vehicles (AUV), single-input-multiple-output (SIMO).

I. INTRODUCTION

Navigation is a key technique for autonomous underwater vehicle (AUV) and other underwater equipment [1], [2]. Most of the underwater explorations including environmental monitoring, disaster prevention, mine reconnaissance, and even military reconnaissance rely on a high-precision position of the AUV [3], [4]. Therefore, achievements on AUV navigation have been gained in the recent decades, and their works can be divided into two categories.

For the first category, several beacons or surface buoys are set to measure the distances between the AUV and beacons, then the AUV's position can be solved using the distance information [5]–[10]. Among these methods, Zhao *et al.* [5] and Caiti *et al.* [6] consider the movement of the beacons during navigation. Moreno-Salinas *et al.* [7] and Liu *et al.* [8] address the problem of optimal beacon placement and time synchronization, respectively. These methods achieve a high navigation precision and work without the aids of other onboard equipment. However, since the navigation depends on several beacons, these methods are restricted by large constructive expending and small effective coverage.

For the second category, single beacon is utilized for AUV's navigation [11]–[16]. These methods need the knowledge of the AUV's inertial navigation system (INS) and depend on several samples obtained in different signal intervals. For example, Tan *et al.* [11] discuss the optimal moving path to decrease the navigation error; Maki *et al.* [12] propose a valid method based on mutual acoustical positioning; Gatsenko *et al.* [13] and Wang *et al.* [14] give the real experiment results.

Besides the distance measurement, other approaches are used to achieve the navigation. Kelner *et al.* [17] propose a ship navigation method utilizing the Doppler effect of the signals transmitted from the costal radio beacons. Xu *et al.* [18] address the navigation via synthetic aperture sonar (SAS) and obtain a much higher navigation precision compared with traditional ultra-short baseline (USBL) navigation system. Bosch *et al.* [19] present a AUV tracking system utilizing light as the medium. The system suffers from a short effective distance.

Inspired by the aforementioned works, we propose a novel navigation method for group AUVs in this paper. Other than the single-input-single-output (SISO) model used by the above methods, we introduce single-input-multiple-output (SIMO) model. Therefore, simultaneous navigation for all AUVs can be achieved in two signal periods, and

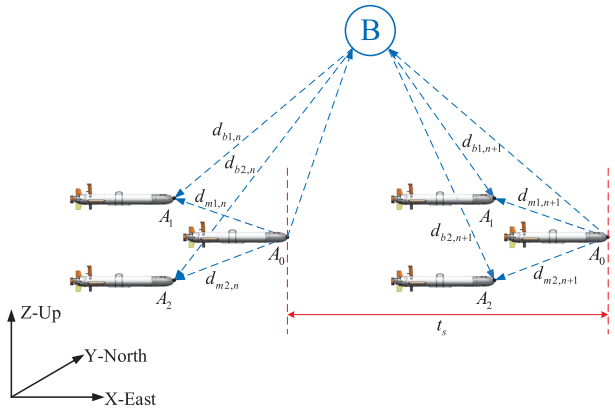

FIGURE 1. Geometrical configuration.

the navigating period is dramatically decreased. Based on the SIMO model, the precision analysis and the tracking method are also presented. The precision analysis tests the robustness against multiple errors and is useful for planning the navigation trajectory. The tracking method based on the extended Kalman filter (EKF) achieves a higher navigation precision and a lower computational burden. Finally, the coordinate fusion algorithm based on the location, error, and time-delay (LED) is presented, which further decreases the navigation error for group AUVs.

In this work, the method is still in theoretical stage, and some simplifications are used. For example, the sound channel is simplified as a homogeneous channel with equal sound speeds and straight sound rays. The time-synchronization error is ignored, and the AUVs are supposed to under the stop-go motion. The method is verified by the simulation results. Our former work will focus on realizing the method and testing the method using real data.

This paper is organized as follows. The navigation method based on SIMO model is proposed in Section II. Precision analysis is conducted in Section III. The tracking method utilizing EKF and coordinate fusion based on LED are presented in Section IV and Section V, respectively. Section VI shows the simulation results, and Section VII concludes our works.

II. SINGLE-BEACON NAVIGATION METHOD FOR GROUP AUVs

A. GEOMETRICAL CONFIGURATION

A typical navigation system for group AUVs is shown in Fig. 1, where, B is the beacon, and $\mathrm{A}_i(i = 0, 1, \ldots, M)$ are the AUVs. The beacon is equipped with global positioning system (GPS) and pressure sensor. The AUVs are equipped with inertial navigation system (INS) and pressure sensor. The GPS and the INS can provide the vehicle's global coordinate, and the pressure sensor can estimate the vehicle's depth. Since the INS has a large accumulative error, it is necessary to implement a beacon based navigation after a long time. Here, we establish the global Cartesian coordinate system as follows. X-axis, Y-axis and, Z-axis indicate the east direction, the north direction, and the up direction, respectively.

B. CONVENTIONAL METHOD BASED ON SISO MODEL

For conventional methods, each AUV and the beacon consist an independent navigation system. The AUV transmits hydroacoustic signals to the beacon. The beacon answers the call, and sends response signals to the AUV. Then, according to [11], the AUV's coordinate can be solved using the time-delay of the signals as

$$2\sqrt{(\mathbf{X}_{i,n} - \mathbf{X}_{b,n}) \cdot (\mathbf{X}_{i,n} - \mathbf{X}_{b,n})^{\mathrm{T}}} = cd_{i,n} \tag{1}$$

where, $d_{i,n}$ is the time-delay of the nth signal transmitted from the beacon to the ith AUV. c is the sound speed. For convenience, the sound speeds are supposed to be the same for different AUVs and different intervals in (1). It is worth noticing that the method can be extend to the situation with different sound speeds, and inhomogeneous sound channels, [20] provides an efficient approach to calculate the equivalent sound speed. $\mathbf{X}_{b,n} = [x_{b,n}, y_{b,n}, z_{b,n}]$ is the beacon's coordinate at discrete time n, where, $[x_{b,n}, y_{b,n}]$ can be calculated from the GPS system, and $[z_{b,n}]$ can be obtained from the pressure sensor. $\mathbf{X}_{i,n} = [x_{i,n}, y_{i,n}, z_{i,n}]$ is the AUV's coordinate at discrete time n. $z_{i,n}$ is known from the AUV's pressure sensor. Although $x_{i,n}$ and $y_{i,n}$ is unknown, their relationship between signals is as

$$\begin{bmatrix} \Delta x_{i,n} \\ \Delta y_{i,n} \end{bmatrix} = \begin{bmatrix} x_{i,n+1} \\ y_{i,n+1} \end{bmatrix} - \begin{bmatrix} x_{i,n} \\ y_{i,n} \end{bmatrix} \tag{2}$$

where, $\Delta x_{i,n}$ and $\Delta y_{i,n}$ is the relative coordinate, and can be calculated from AUV's INS ([21]–[23]).

Using time-delays from two signal intervals, and substitute (2) into (1), $[x_{i,n}, y_{i,n}]$ is solved, and the navigation is achieved. Hence, the navigation period for single AUV is $2t_s$, where, t_s is the signal interval. Considering the beacon can answer only one call in each signal period to avoid aliasing, the navigation period for the whole system should be $2Mt_s$, where M is the number of the AUVs. Compared with the period for single AUV, it can be seen that the conventional group AUVs' navigation system suffers from a much longer navigating period. Besides, the navigation times for each AUV are not the same, which will lead to a big problem in the following coordinate fusion process.

C. NEW METHOD BASED ON MISO MODEL

To avoid the aforementioned disadvantages, we propose a novel single-beacon navigation method for group AUVs based on SIMO model in this sub-section. As shown in Fig. 1, the SIMO model means that only single AUV transmits the signal in the navigation system, and the other multiple AUVs receive the signal. Without losing the generalization, we suppose A_0 as the AUV send the signal. Then, each other AUV $\mathrm{A}_i(i = 1, 2, \ldots, N)$ can receive two signals as

$$\sqrt{(\mathbf{X}_{i,n} - \mathbf{X}_{b,n}) \cdot (\mathbf{X}_{i,n} - \mathbf{X}_{b,n})^{\mathrm{T}}} + \sqrt{(\mathbf{X}_{0,n} - \mathbf{X}_{b,n}) \cdot (\mathbf{X}_{0,n} - \mathbf{X}_{b,n})^{\mathrm{T}}} = cd_{bi,n} \tag{3}$$

$$\sqrt{(\mathbf{X}_{i,n} - \mathbf{X}_{0,n}) \cdot (\mathbf{X}_{i,n} - \mathbf{X}_{0,n})^{\mathrm{T}}} = cd_{mi,n} \tag{4}$$

TABLE 1. Parameters for case 2.

Standard deviation of the time-delay	Standard deviation of the INS	Standard deviation of the sound speed	Standard deviation of the beacons coordinate	Standard deviation of the depth
0.3 ms	0.2%	2 m/s	1.5 m/s	1 m
Sound speed	Velocity of the AUVs	Heading of the AUVs (related to X axis)	Velocity of the beacon	Length of the virtual baseline
1500 m/s	2 m/s	[5 degree, -5 degree]	0 m/s	200 m

where, $d_{bi,n}$ is the time-delay of the signal passed by the beacon B, $d_{mi,n}$ is the time-delay of the signal directly from A_0.

It can be seen from (3) and (4), that the equations contains four unknowns ($x_{i,n}$, $y_{i,n}$, $x_{0,n}$, and $y_{0,n}$). Therefore, time-delays from two signals are required to solve the coordinates. Compared with the conventional method based on SISO model, new method based on SIMO model has the following advantages:

1) The navigation precision is increased.

2) All AUVs can be navigated in two signal intervals ($2t_s$). The navigating period is dramatically decreased.

3) All AUVs can be navigated at the same time. Therefore, it is possible to do the coordinate fusion, which can fuse all the independently measured AUVs' coordinates to consist a holistic coordinate system.

4) The new method releases from fuzzy solution, which is a serious problem in the conventional SISO model.

5) The receivers keep silence during the navigation, which enhances the concealment of the AUVs.

III. PRECISION ANALYSIS

In this section, we put forward precision analysis to evaluate the proposed navigation method, and horizontal dilution of precision (HDOP) is introduced as the criterion. The definition of HDOP is given as

$$\mathrm{HDOP} = \sqrt{g_{xi}^2 + g_{yi}^2} \tag{5}$$

where, g_{xi} and g_{yi} are the X coordinate error and Y coordinate error for AUV A_i, respectively.

For the scene discussed in this paper, the errors may come from five aspects, which are: 1) error of the measured time-delay, 2) error of the INS coordinate, 3) error of the beacon's coordinate, 4) error of the measured sound velocity, 5) error of the measured depth. The statistical property between these errors and the HDOP can be described as

$$\begin{aligned}\mathbf{D}_i = \mathbf{M}_i^{-1} \cdot \{&\mathbf{M}_\mathrm{T} \cdot \mathbf{D}_\mathrm{T} \cdot \mathbf{M}_\mathrm{T}^\mathrm{T} + \mathbf{M}_\mathrm{INS} \cdot \mathbf{D}_\mathrm{INS} \cdot \mathbf{M}_\mathrm{INS}^\mathrm{T} \\ &+ \mathbf{M}_\mathrm{B} \cdot \mathbf{D}_\mathrm{B} \cdot \mathbf{M}_\mathrm{B}^\mathrm{T} + \mathbf{M}_\mathrm{C} \cdot \mathbf{D}_\mathrm{C} \cdot \mathbf{M}_\mathrm{C}^\mathrm{T} \\ &+ \mathbf{M}_\mathrm{H} \cdot \mathbf{D}_\mathrm{H} \cdot \mathbf{M}_\mathrm{H}^\mathrm{T}\} \cdot \mathbf{M}_i^{-1\mathrm{T}}\end{aligned} \tag{6}$$

where, $(*)^\mathrm{T}$ means the transpose of the matrix. $\mathbf{D}_i$, $\mathbf{D}_\mathrm{T}$, $\mathbf{D}_\mathrm{INS}$, $\mathbf{D}_\mathrm{B}$, $\mathbf{D}_\mathrm{C}$, and $\mathbf{D}_\mathrm{H}$ are the covariance matrixes for AUV's coordinate, the measured time-delay, the INS, the beacon's coordinate, the sound speed, and the depth, respectively, and we have $\mathrm{HDOP} = \sqrt{\mathbf{D}_i(1,1) + \mathbf{D}_i(2,2)}$. $\mathbf{M}_i$, $\mathbf{M}_\mathrm{T}$, $\mathbf{M}_\mathrm{INS}$, $\mathbf{M}_\mathrm{B}$, $\mathbf{M}_\mathrm{C}$, and $\mathbf{M}_\mathrm{H}$ are the corresponding partial differential matrixes. Detailed derivation of (6) is given in Appendix A, together with the expression of the matrixes.

From (6), it can be seen that the precision of the navigation method based on SIMO is influenced not only by the error parameters ($\mathbf{D}_i$, $\mathbf{D}_\mathrm{T}$, $\mathbf{D}_\mathrm{INS}$, $\mathbf{D}_\mathrm{B}$, $\mathbf{D}_\mathrm{C}$, $\mathbf{D}_\mathrm{H}$), but also by the scenario configuration parameters ($\mathbf{M}_i$, $\mathbf{M}_\mathrm{T}$, $\mathbf{M}_\mathrm{INS}$, $\mathbf{M}_\mathrm{B}$, $\mathbf{M}_\mathrm{C}$, $\mathbf{M}_\mathrm{H}$). That is to say, the output navigation error is decided by the input error parameters (such as the time-delay error, the INS error, the beacon's coordinate error, the sound speed error, the depth error) and the scene parameters (such as the geometrical configuration, the motional differentiation of the AUVs, the length of the virtual baseline). Firstly, we use the following cases to show the influence of the scene parameters.

Case 1): The sender A_0 has the same velocity with the receivers ($A_i (i = 1, 2, .., M)$).

In this case, (4) for different signal intervals is same, and the navigation becomes a singular parabolic problem. In view of precision analysis, since the partial differential matrix for AUV's coordinate (M_i) is noninvertible, the calculated covariance matrix of AUV's coordinate (D_i) is infinite. Therefore, the coordinates of the AUVs cannot be solved. Case 1 indicates that to achieve the navigation for group AUVs, the sender and the receiver mush have different velocities.

Case 2): The sender A_0 and the receivers $A_i (i = 1, 2, .., M)$ have different velocities.

In case 2, there are two AUVs (one is the sender and the other is the receiver), and the parameters are listed in Table. 1. Trajectory of the AUV is shown in Fig. 2(a), and the corresponding precision is shown in Fig. 2(b). Case 2 shows that the SIMO model achieves the navigation for group AUVs, and obtains a navigation precision better than 6 m in the given parametric environment.

Case 3): The sender A_0 and the receivers $A_i (i = 1, 2, .., M)$ have different velocities with a larger heading difference.

In this case, scene parameters are the same with case 2 (Table 1) except the AUVs' heading. The heading of A_0 and A_1 are -15 degrees and 15 degrees respectively. Trajectories of the AUVs are shown in Fig. 3(a), and the corresponding precision is shown in Fig. 3(b), from which, the navigation precision is better than 5 m. Case 3 indicates that the navigation precision increases with a larger difference between AUVs' velocities.

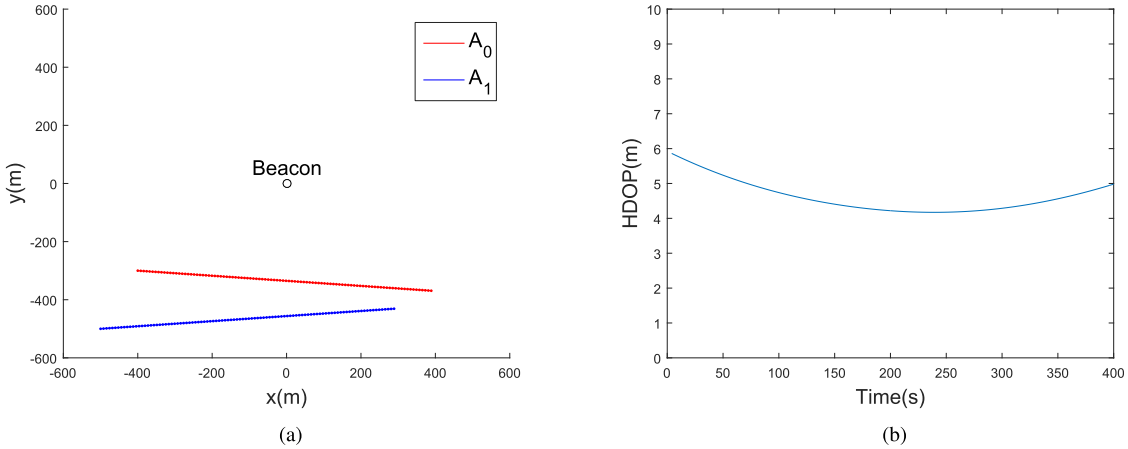

FIGURE 2. Precision analysis for case 2. (a) AUVs' trajectories. (b) Navigation precision.

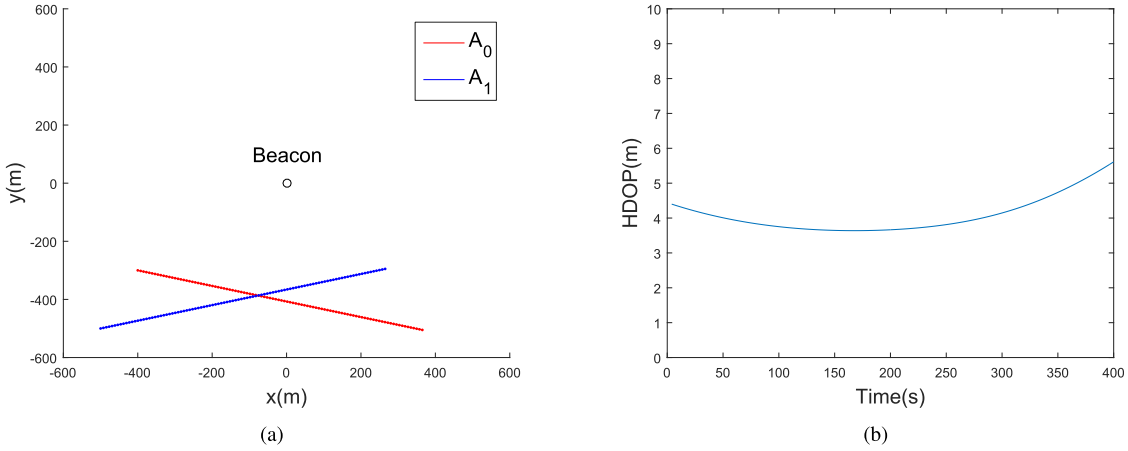

FIGURE 3. Precision analysis for case 3. (a) AUVs' trajectories. (b) Navigation precision.

Case 4): The sender A_0 and the receivers $A_i (i = 1, 2, .., M)$ have different velocities with a longer virtual baseline.

The scene parameters are the same with case 2 (Table 1) except the length of the virtual baseline. In this case, the virtual baseline length is 320 m. Trajectories of the AUVs are the same with Fig. 3(a), and the navigation precision is shown in Fig. 4. Compared with Case 2, the navigation precision is improved to about 4 m, which indicates that the navigation precision increases with a larger virtual baseline length. Combining Case 2-4, it also shows that the navigation method has a better precision when the AUVs are near the beacon.

Next, we will exam the method's robustness against the input errors including the time-delay error, the INS error, the beacon's coordinate error, the sound speed error, and the depth error. The results are shown in Fig. 5.

From Fig. 5, the navigation method based on SIMO has a good robustness against the INS error, a moderate robustness against the sound speed error and the beacon's coordinate error, and a poor robustness against the time-delay error and the depth error.

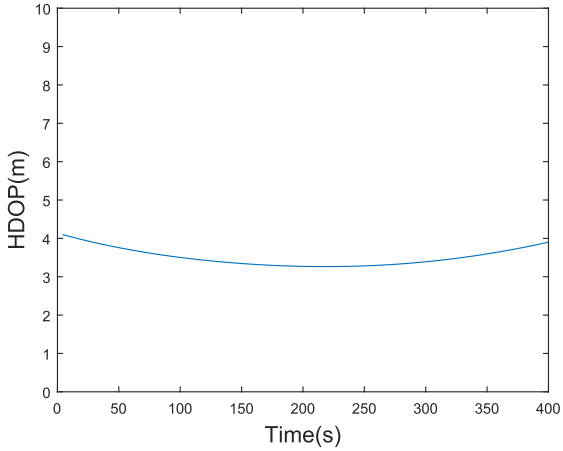

FIGURE 4. Precision analysis for Case 4.

Overall, the navigation method based on SIMO model for group AUVs has the following characters:

1) The navigation precision increases with a greater difference between the AUVs' velocity. Specifically, when the

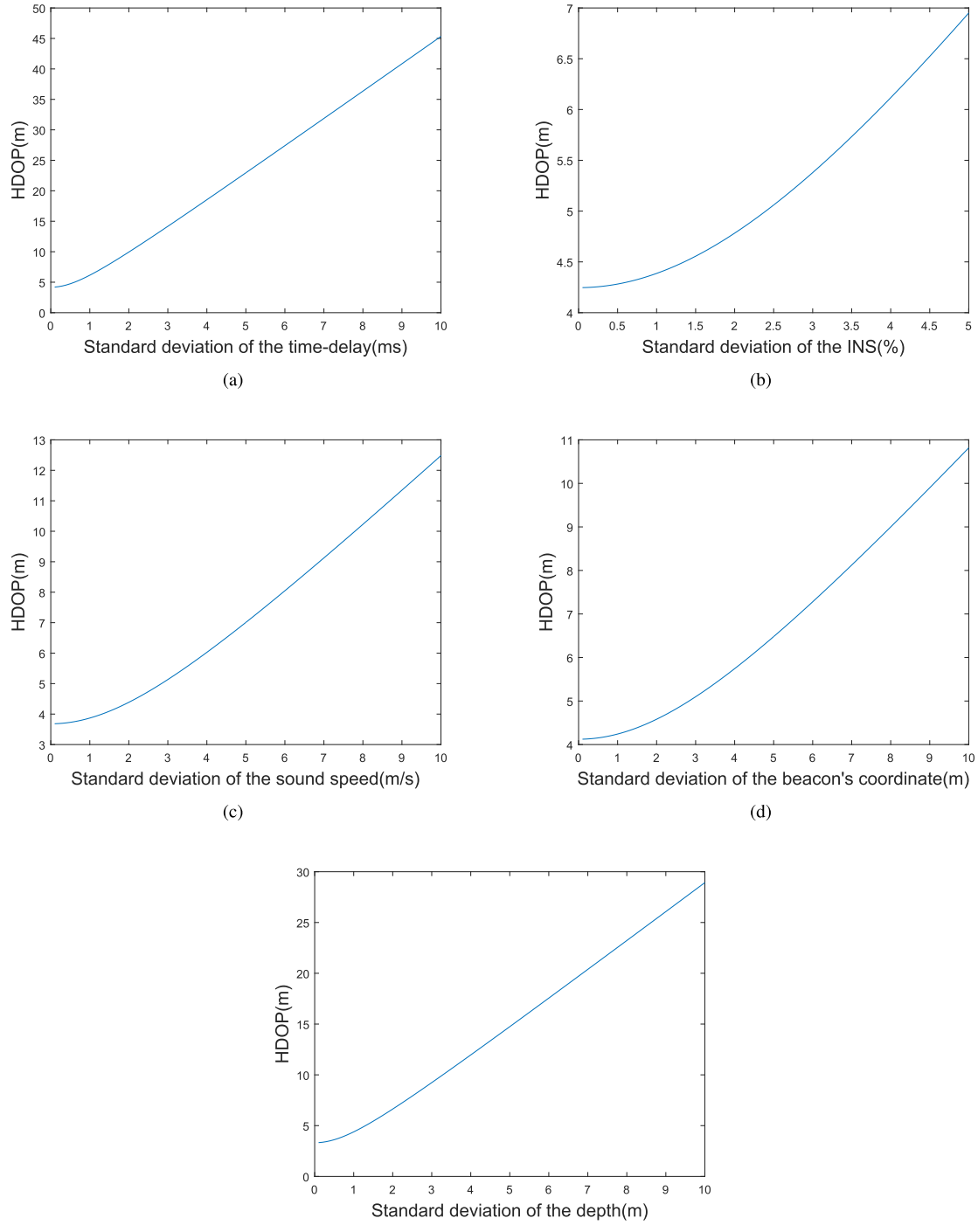

FIGURE 5. Robustness analysis against input errors. (a) time-delay error. (b) INS error. (c) Sound speed error. (d) Beacons coordinate error. (e) Depth error.

AUVs' velocities are the same, the navigation error becomes infinity.

2) The navigation precision is sensitive with the AUV's location. Usually, a near distance between the AUVs and the beacon results a higher navigation precision.

3) The navigation precision is sensitive with the length of the virtual baseline length, and a longer virtual baseline results a higher navigation precision.

4) As predicted, the navigation error grows with the factor's error. The growth degrees are not the same for different factors. The method has a high robustness against the INS error, a moderate robustness against the sound speed error and the beacon's coordinate error, but a poor robustness against the time-delay error and the depth error.

Above precision analysis can be used in planning the best trajectory for navigation, and guide the design of a

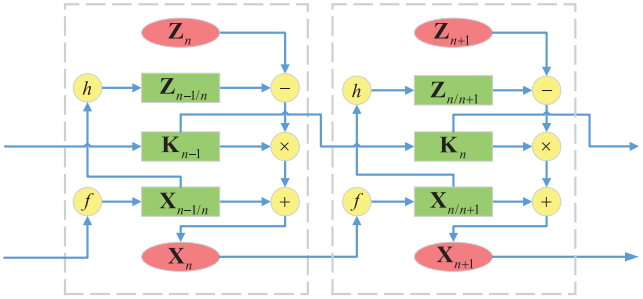

FIGURE 6. Structure of the EKF.

real navigation system. Generally speaking, a high navigation precision (better than 5 m) requires a great difference between AUV's velocities (heading difference larger than 30 degree or equivalent velocity difference), a suitable distance from the beacon (lower than 1000 m), and an appropriate virtual baseline (longer than 200 m). The navigation system needs a high precision time-delay estimation algorithm (1 ms) and a high precision pressure sensor (1.5 m), but does not need to pay much cost on increasing the estimation precision of the INS (2.5%), the beacon's coordinate (2.5 m), and the sound speed (3 m/s).

IV. TRACKING METHOD UTILIZING EKF

The proposed single-beacon navigation method based on SIMO model can achieve short time and a large number of navigation for group AUVs. The method is proved to have a high precision for two time-delay samples. However, for a long time navigation, a large number of time-delay samples can be obtained. Under such circumstance, a tracking method based on the SIMO model is proposed in this section. By utilizing EKF ([24], [25]), the proposed tracking method can achieve a lower computing burden and a better precision compared with the proposed navigation method.

EKF is a non-linear filter proposed in 1970s, and has been widely used in recent years. The basic principle for EKF is utilizing the system observation to amend the system state. Hence, after a long time observing, the error of the system state can infinitely approach the Cramer-Rao bound. The structure of EKF is shown in Fig. 6, where, $\mathbf{X}_n$ is the state vector, $\mathbf{Z}_n$ is the observation vector, $\mathbf{K}_n$ is the gain matrix, f is the state transition function, and h is the observation function.

Here, we establish the EKF model for group AUVs' navigation method based on SIMO. The state vector, the observation vector, the state transition function, and the observation function are as follows, (7)–(10) shown at the bottom of this page, where, $v_i(i = 0, 1, \ldots, M)$ is the speed of the AUV; $\varphi_i(i = 0, 1, \ldots, M)$ is the heading of the AUV; $\theta_i(i = 0, 1, \ldots, M)$ is the pitch angle of the AUV. $\mathbf{U}_n = [v_0, \varphi_0, \theta_0, v_i, \varphi_i, \theta_i]^{\mathrm{T}}$ is the control vector.

The observability is a significant precondition for a designed observation system. Therefore, the observability analysis is presented based on the Lie derivative ([26], [27]). Including 0th and 1th order Lie derivative, the observability matrix is given as

$$\begin{aligned} \mathrm{O}' = [&\nabla L^0 h_0, \nabla L^1_{f_1} h_0, \nabla L^1_{f_2} h_0, \nabla L^1_{f_3} h_0, \nabla L^1_{f_4} h_0, \\ &\nabla L^1_{f_5} h_0, \nabla L^1_{f_6} h_0, \nabla L^0 h_1, \nabla L^1_{f_1} h_1, \nabla L^1_{f_2} h_1, \\ &\nabla L^1_{f_3} h_1, \nabla L^1_{f_4} h_1, \nabla L^1_{f_5} h_1, \nabla L^1_{f_6} h_1] \end{aligned} \tag{11}$$

where, $f_1 = \frac{\partial \hat{\mathbf{X}}}{\partial v_0}$, $f_2 = \frac{\partial \hat{\mathbf{X}}}{\partial \varphi_0}$, $f_3 = \frac{\partial \hat{\mathbf{X}}}{\partial \theta_0}$, $f_4 = \frac{\partial \hat{\mathbf{X}}}{\partial v_i}$, $f_5 = \frac{\partial \hat{\mathbf{X}}}{\partial \varphi_i}$, and $f_6 = \frac{\partial \hat{\mathbf{X}}}{\partial \theta_i}$. $h_0 = \frac{\sqrt{[x_i-x_b]^2+[y_i-y_b]^2+[z_i-z_b]^2}}{c} + \frac{\sqrt{[x_0-x_b]^2+[y_0-y_b]^2+[z_0-z_b]^2}}{c}$. $h_1 = \frac{\sqrt{[x_i-x_0]^2+[y_i-y_0]^2+[z_i-z_0]^2}}{c}$. Detailed expression of O' is given in Appendix B.

From (11), it can be seen that: $rank(O') = 3$, unless $v_0 = v_i = 0$. As an example, consider the special case, in which, trajectories for the sender and the receiver are the same. Even under such extremely disadvantageous circumstance, we have $\nabla L^1_{f_1} h_0 = [2, 0, 0, 0]^{\mathrm{T}}$, $\nabla L^1_{f_2} h_0 = [0, 2v_0, 0, 0]^{\mathrm{T}}$, $\nabla L^1_{f_4} h_0 = [0, 0, 2, 0]^{\mathrm{T}}$, $\nabla L^1_{f_5} h_0 = [0, 0, 0, 2v_i]^{\mathrm{T}}$, and $rank(O') = 3$. That is to say, the established observation system is always observable for any moving AUVs.

It is worth noticing that EKF is one of the most efficient and widely used tracking algorithms. It is clearly possible to use more sophisticated non-linear filters, such as the cubature Kalman filter [28] or the particle filter [29]. These techniques may lead to some precision improvement, but the computational burdens are also increased, and this analysis is beyond the scope of this paper.

$$\mathbf{X}_n = [x_{0,n}, y_{0,n}, x_{i,n}, y_{i,n}]^{\mathrm{T}} \tag{7}$$

$$\mathbf{Z}_n = [d_{bi,n}, d_{mi,n}]^{\mathrm{T}} \tag{8}$$

$$\mathbf{X}_{n+1} = f(\mathbf{X}_n, \mathbf{U}_n) = \mathbf{X}_n + \begin{bmatrix} v_0 cos\varphi_0 cos\theta_0 \\ v_0 \sin\varphi_0 cos\theta_0 \\ v_i cos\varphi_i cos\theta_i \\ v_i \sin\varphi_i cos\theta_i \end{bmatrix} t_s \tag{9}$$

$$\mathbf{Z}_n = h(\mathbf{X}_n) = \begin{bmatrix} \frac{\sqrt{(\mathbf{X}_{i,n} - \mathbf{X}_{b,n}) \cdot (\mathbf{X}_{i,n} - \mathbf{X}_{b,n})^{\mathrm{T}}} + \sqrt{(\mathbf{X}_{0,n} - \mathbf{X}_{b,n}) \cdot (\mathbf{X}_{0,n} - \mathbf{X}_{b,n})^{\mathrm{T}}}}{c} \\ \frac{\sqrt{(\mathbf{X}_{i,n} - \mathbf{X}_{0,n}) \cdot (\mathbf{X}_{i,n} - \mathbf{X}_{0,n})^{\mathrm{T}}}}{c} \end{bmatrix} \tag{10}$$

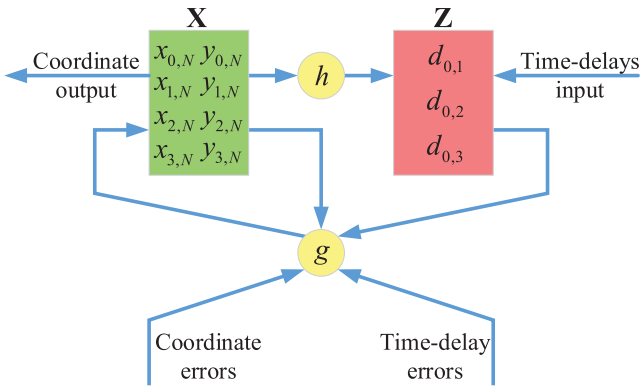

FIGURE 7. Coordinates fusion based on LED.

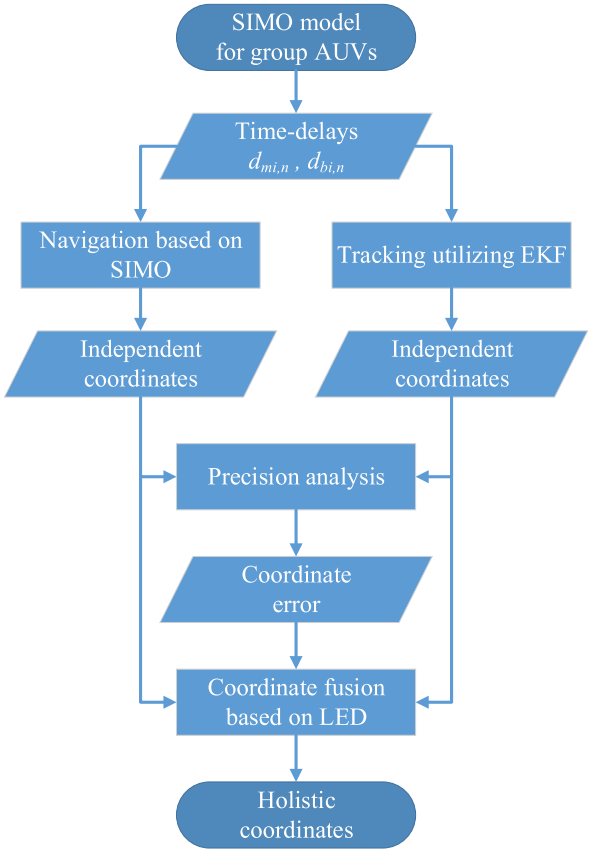

FIGURE 8. Flow chart for the method.

V. COORDINATE FUSION BASED ON LED

After navigation or tracking, AUVs' coordinate for the last sample is obtained as $\mathbf{X}_{i,N}(i = 1, 2, \ldots, N)$. However, since the receivers are independent from each other, and the navigation precisions for each receiver are not the same, it is necessary to fuse the coordinates and form a holistic coordinate system. Therefore, a coordinate fusion method based on LED (location, error, and time-delay) is proposed in this section. Utilizing the measured locations, calculated errors, and the time-delays of the signal between the AUV's, the proposed method can achieve the coordinate fusion with lower navigation errors.

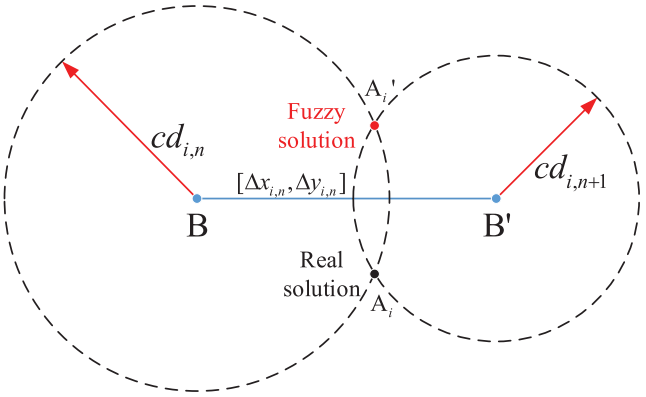

FIGURE 9. Schematic diagram for fuzzy solution.

Considering the receives are silent with each other during the navigation, a hydroacoustic data exchange should be implemented to report their own locations after navigation. Through the exchange signal, the signal's time-delay, which indicates the distance between AUVs, can be measured. For example, if A_0 is interested with other AUVs' coordinates, $A_i(i = 1, 2, \ldots, N)$ should report their measured coordinates to A_0 (by modulating the coordinates in the frequency of the transmitted signal). Generally speaking, not all AUVs need to be aware of each other AUVs' positions. However, at least one AUV should know the coordinate of the other AUVs to monitor the situation of the AUVs group. Hence, the minimized time interval for information exchange between AUVs is t_s. Appling the precision analysis in Section III, prior information (HDOP from (6)) about the coordinate errors can also be calculated. Based on the above information (measured coordinate, time-delays of the signals, prior information about the coordinate errors), the coordinate fusion method based on LED is given in Fig. 7 (suppose $M = 3$), where, $\mathbf{x}$ is the state vector, $\mathbf{Z}$ is the observation vector, h is the observation function, g is the update function. $d_{i1,i2}$ means the time-delay between A_{i1} and A_{i2} (for example, $d_{0,1}$ is the time-delay between A_0 and A_1).

Detailed procedures are as follows:

Step 1: The initial value of the state vector is set to be the measured coordinates.

$$\mathbf{X}_1 = [x_{0,N}, y_{0,N}, x_{1,N}, y_{1,N}, x_{2,N}, y_{2,N}, x_{3,N}, y_{3,N}]^{\mathrm{T}} \quad (12)$$

Step 2: Predict the observation vector through observation function.

$$\mathbf{Z}_k = h(\mathbf{X}_k) = \begin{bmatrix} \frac{\sqrt{[x_{0,N}-x_{1,N}]^2+[y_{0,N}-y_{1,N}]^2+[z_{0,N}-z_{1,N}]^2}}{c} \\ \frac{\sqrt{[x_{0,N}-x_{2,N}]^2+[y_{0,N}-y_{2,N}]^2+[z_{0,N}-z_{2,N}]^2}}{c} \\ \frac{\sqrt{[x_{0,N}-x_{3,N}]^2+[y_{0,N}-y_{3,N}]^2+[z_{0,N}-z_{3,N}]^2}}{c} \end{bmatrix} \quad (13)$$

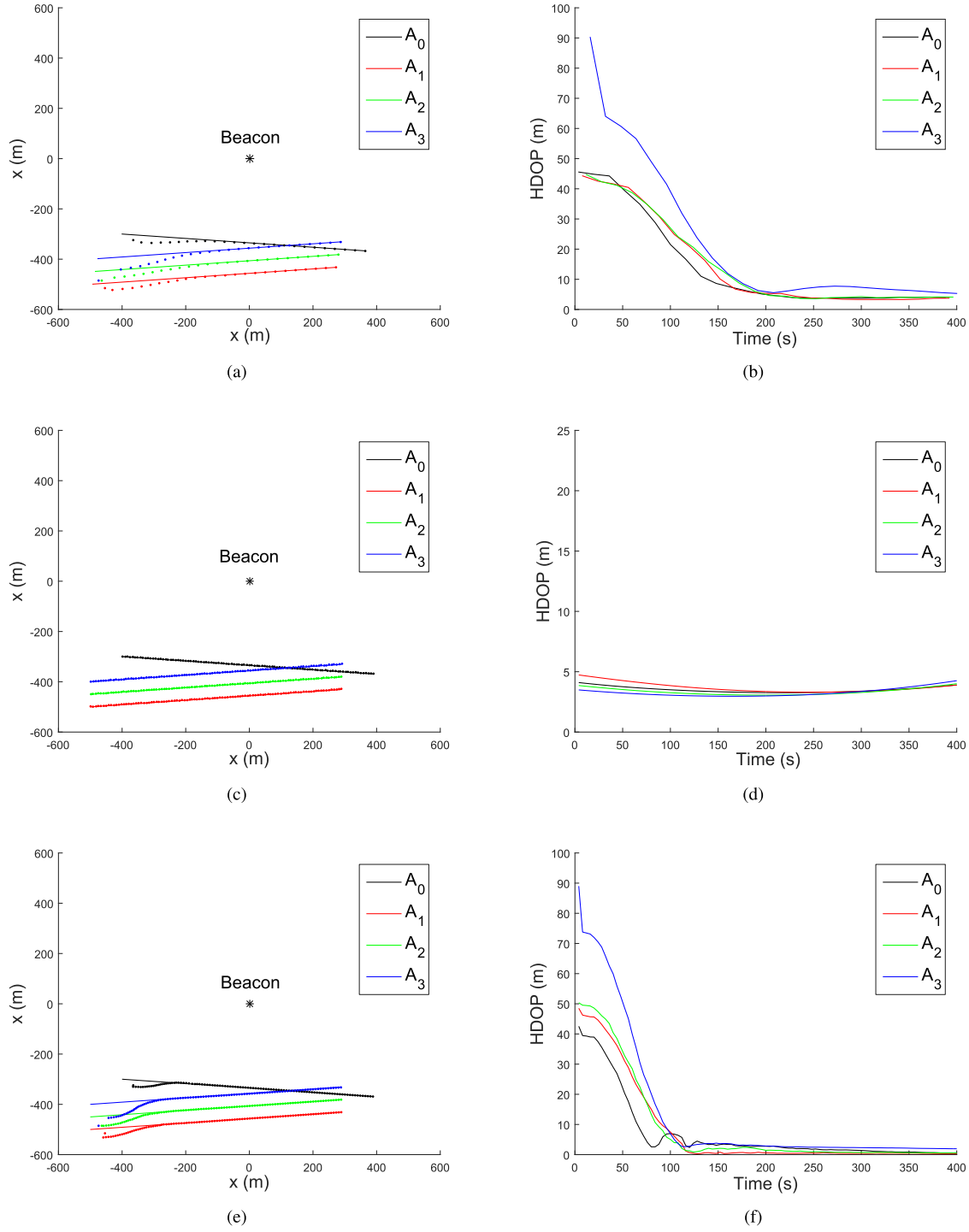

FIGURE 10. Navigation or tracking results for simulation 2. (a) Result of the tracking method based on SISO model. (b) Precision of the tracking method based on SISO model. (c) Result of the navigation method based on SIMO model. (d)Precision of the navigation method based on SIMO model. (e) Result of the tracking method utilizing EKF based on SIMO model. (f) Precision of the tracking method utilizing EKF based on SIMO model.

Step 3: Calculate the distance between predicted observation and real observation.

$$\hat{\mathbf{Z}}_k = \mathbf{Z}_k - \mathbf{Z} = \mathbf{Z}_k - \begin{bmatrix} d_{0,1} \\ d_{0,2} \\ d_{0,3} \end{bmatrix} \tag{14}$$

Step 4: Update the state vector through update function.

$$\begin{aligned} \mathbf{X}_{k+1} &= g(\mathbf{X}_k, \hat{\mathbf{Z}}_k, \mathbf{D}, \mathbf{R}) \\ &= \mathbf{X}_k + \mathbf{H}_k^{\mathrm{T}} \cdot (\mathbf{H}_k \cdot \mathbf{D} \cdot \mathbf{H}_k^T + \mathbf{R})^{-1} \cdot \hat{\mathbf{Z}}_k \end{aligned} \tag{15}$$

TABLE 2. Performance for Simulation 1.

	SISO model [transmitter, receiver, receiver]	MISO model [transmitter, receiver, receiver]
Real solution percentage	[74.3%, 67.1%, 83.5%]	[100%, 100%, 100%]
Theoretically coordinate error	[8.24m, 7.31m, 5.57m]	[6.37m, 6.02m, 4.76m]
Simulation coordinate error	[8.96m, 8.23m, 6.66m]	[7.03m, 5.50m, 5.01m]

TABLE 3. Performance for Simulation 2.

	Tracking method based on SISO model	Navigation method based on SIMO model	Tracking method utilizing EKF based on SIMO model	Coordinate fusion method based on LED
Coordinate error (average value)	5.93 m	4.23 m	1.77 m	1.01 m
Computing time	0.011 s	0.094 s	0.016 s	-
Period	16 s	8 s	4 s	-

where, $\mathbf{D} = \text{diag}(\sigma^2_{x_{0,N}}, \sigma^2_{y_{0,N}}, \sigma^2_{x_{1,N}}, \sigma^2_{y_{1,N}}, \sigma^2_{x_{2,N}}, \sigma^2_{y_{2,N}}, \sigma^2_{x_{3,N}}, \sigma^2_{y_{3,N}})$ is the covariance matrix of AUV's coordinate calculated from (6), $\mathbf{R} = \text{diag}(\sigma^2_{d_{0,1}}, \sigma^2_{d_{0,2}}, \sigma^2_{d_{0,3}})$ is the covariance matrix of the measured time-delay, $\mathbf{H}_k = \frac{\partial h}{\partial \mathbf{X}}|\mathbf{x}_k$ is the partial differential matrix for AUV's coordinate.

Step 5: Loop step 2 to step 4, until the difference between two adjacent loops is lower than a threshold, and the coordinates after fusion equal to the $\mathbf{X}_k$ in the final loop.

Overall, flow chart for the proposed single beacon navigation method for group AUVs based on SIMO model is as shown in Fig. 8.

VI. SIMULATION RESULTS

A. SIMULATION 1

This simulation is presented to verify the precision analysis and illustrate the fuzzy solution problem for the conventional SISO model. Three AUVs are established. One is the transmitter with the speed 2.5 m/s, and the others are the with the speed 2 m/s (for the SISO model, each AUV is both the transmitter and the receiver). The headings of the AUVs are all 0 degree. The other parameters are the same with Table 1. The relative coordinates of the AUVs (to the beacon) are [0 m, 300 m, −30 m], [0 m, 250 m, −30 m], and [0 m, 350 m, −30 m], respectively. The initialized coordinates are distributed in a circle, with the real coordinate as the center, and 500 m as the radius. Applying the conventional method based on SISO model and the proposed method based on SIMO model, the navigation performance is obtained from the average of 1000 simulation runs as shown in Table 2.

In Table 2, the simulation coordinate error coincides with the theoretically coordinate error, and it proves the correctness of the precision analysis in Section III. Table 2 also indicates that the conventional method based on SISO model suffers from fuzzy solution. Fig. 9 investigates the reason for the fuzzy solution. Here we consider a stationary AUV and a moving beacon (B to B'). The solution A_i should satisfy (1), and subsequently locates at the intersection of the two circles. Since there are two intersections, the solution may converge to a wrong coordinate A'_i, if the initialized coordinate is improperly selected. However, for the SIMO model, there is no such fuzzy solution simultaneously satisfying equations (3)-(4). Therefore, the SIMO model releases from fuzzy solution, and the real solution percentage can reach 100%.

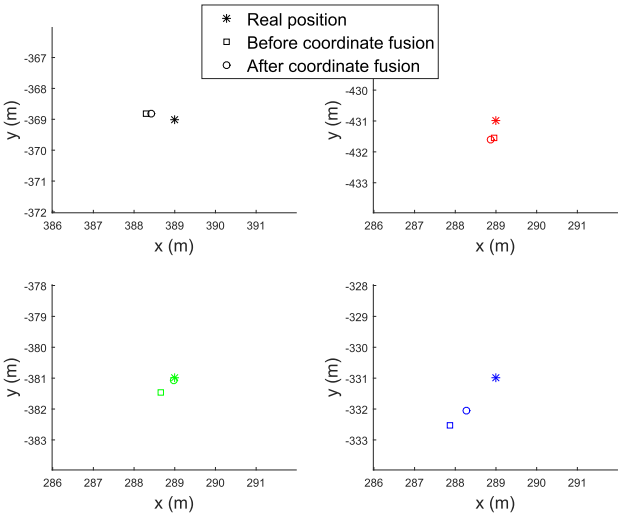

FIGURE 11. Coordinate fusion result for simulation 2.

B. SIMULATION 2

This simulation is presented to show the whole procedure of the proposed SIMO model, and compare its performance with the conventional SISO model. Four AUVs' trajectories are synthetic as follows. Speeds of the AUVs are 2 m/s. Headings of the sender (A_0) and the receivers (A_1, A_2, and A_3) are -5 degrees and 5 degrees, respectively. Signal interval is 4 s and the virtual baseline is 320 m. The whole navigation duration is 400 s. Sound speed and the errors are shown as Table 1.

Appling the tracking method based on conventional SISO model, the navigation method based on SIMO model, and the tracking method based on SIMO model, the results are shown in Fig. 10. Fig. 10(a), Fig. 10(c), and Fig. 10(e) show the navigation or tracking trajectories, where, the solid lines show the real position of the target, and the dot line show the estimated results. Fig. 10(b), Fig. 10(d), and Fig. 10(f) show the corresponding errors. After tracking, coordinate fusion

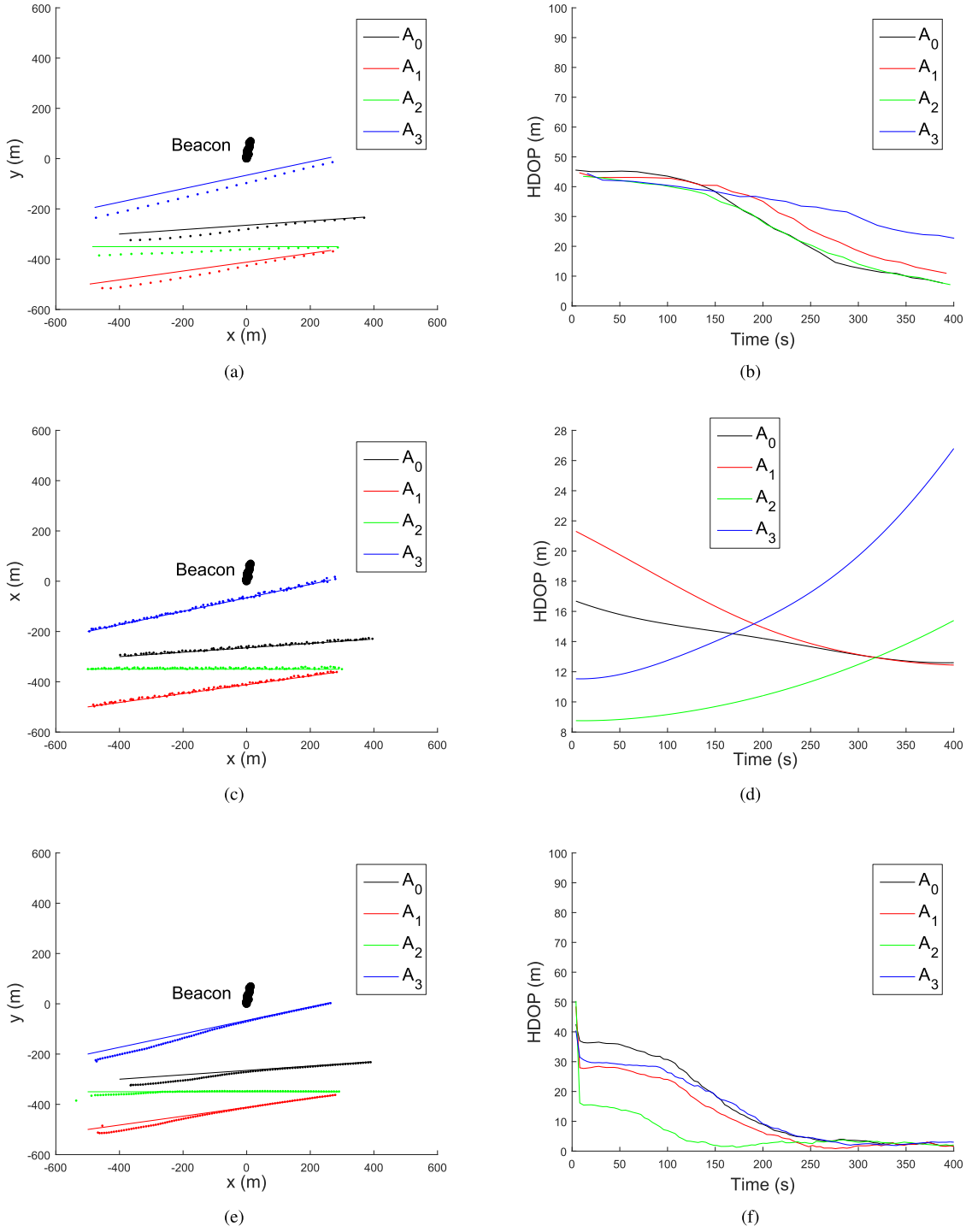

FIGURE 12. Navigation or tracking results for simulation 3. (a) Result of the tracking method based on SISO model. (b) Precision of the tracking method based on SISO model. (c) Result of the navigation method based on SIMO model. (d)Precision of the navigation method based on SIMO model. (e) Result of the tracking method utilizing EKF based on SIMO model. (f) Precision of the tracking method utilizing EKF based on SIMO model.

based on LED is put forward, and the final result is shown in Fig. 11. Table 3 lists the performance of these methods.

From the figures and the table, it can be seen that:

1) Compared with the conventional method based on SISO model, the new method based on SIMO model has shorter periods, and higher precisions. Especially for the tracking method, since the period is dramatically reduced, more observations are obtained in the same time, and it is faster for the tracking error to converge to the Cramer-Rao lower bound.

TABLE 4. Performance for Simulation 3.

	Tracking method based on SISO model	Navigation method based on SIMO model	Tracking method utilizing EKF based on SIMO model	Coordinate fusion method based on LED
Coordinate error (average value)	19.92 m	12.15 m	6.33 m	4.96 m
Computing time	0.012 s	0.093 s	0.016 s	-
Period	16 s	8 s	4 s	-

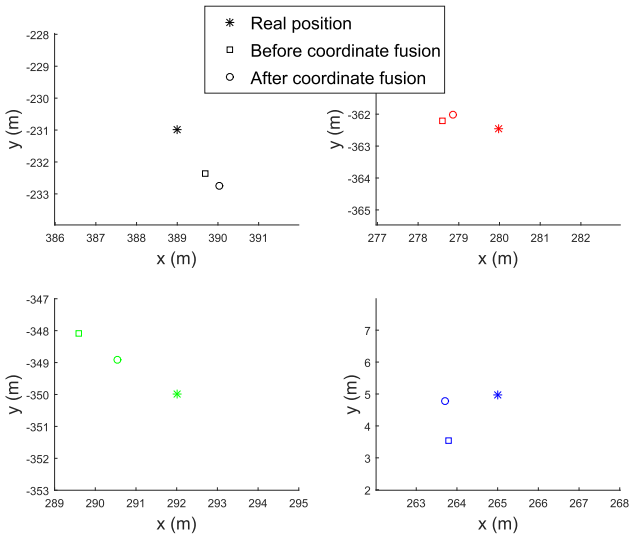

FIGURE 13. Coordinate fusion result for simulation 2.

2) Compared with navigation method based on SIMO model, the tracking method utilizing EKF decreases the computational burden and the HDOP. However, the tracking method needs a convergent period (about 100 s in simulation 2. Hence, it is suitable for a long time observation.

3) After coordinate fusion based on LED, the independent coordinates for each AUV become a holistic coordinate system, and the total coordinate error is further decreased.

C. SIMULATION 3

This simulation is presented based on a more complicated environment, which is closer to the real situation. The time-synchronization error is considered, and we set it as 1 ms. The AUVs are with different velocities, their headings are 0 degrees, 5 degrees, 10 degrees, and 15 degrees respectively. The beacon moves with the sea flow with a speed of 0.3 m/s. Other parameters are the same with simulation 2.

The results are given in Figs. 12-13 and Table 4. Fig. 12 shows the result and precision for the tracking method based on SISO model, the navigation method based on MISO model, and the tracking method utilizing EKF. Fig. 13 shows the coordinate fusion result. Table 4 shows the comparison of the performance.

Due to the time-synchronization error, navigation or tracking precision are dramatically decreased. Especially for the conventional method based on SISO model, the average tracking error is about 20 m. For the proposed SIMO model, the coordinate error for navigation and tracking are about 12 m and 6 m, respectively, which indicates that the proposed SIMO model has a better robustness against the time-synchronization error compared with the conventional SISO model.

These simulation results coincide with the theoretical analysis, and prove the effectiveness of the proposed methods.

VII. CONCLUSION AND FUTURE WORK

In this paper, a novel navigation method for group AUVs based on SIMO model is proposed. Using the time-delay of the signal forwarded by the beacon and the time-delay of the signal directly from the sender, the method can achieve simultaneous and high precision navigation for all receivers. Precision analysis indicates that higher navigation precision can be obtained with a great difference between AUV's velocities, a suitable distance from the beacon, an appropriate virtual baseline and a high precision time-delay and depth estimation algorithm. Based on the SIMO model, we also propose a tracking method utilizing EKF, which has a smaller computing time and a higher precision, but needs a long observing time compared with the navigation method. Finally, a coordinate fusion method based on LED is proposed. The method combines the independent coordinates to a holistic coordinate system, and the coordinate error is reduced. Simulation results correspond with the theoretically analysis, and show the effectiveness of the proposed method.

APPENDIX A
DERIVATION OF (6)

Calculating the partial differential equation for (3)-(4), we have:

$$\mathbf{M}_i \cdot \begin{bmatrix} \mathrm{d}x_{0,n} \\ \mathrm{d}y_{0,n} \\ \mathrm{d}x_{i,n} \\ \mathrm{d}y_{i,n} \end{bmatrix} + \mathbf{M}_\mathrm{T} \cdot \begin{bmatrix} \mathrm{d}d_{bi,n} \\ \mathrm{d}d_{mi,n} \\ \mathrm{d}d_{bi,n+1} \\ \mathrm{d}d_{mi,n+1} \end{bmatrix} + \mathbf{M}_\mathrm{INS} \cdot \begin{bmatrix} \mathrm{d}\Delta x_{0,n} \\ \mathrm{d}\Delta y_{0,n} \\ \mathrm{d}\Delta x_{i,n} \\ \mathrm{d}\Delta y_{i,n} \end{bmatrix}$$
$$+ \mathbf{M}_\mathrm{B} \cdot \begin{bmatrix} \mathrm{d}x_{b,n} \\ \mathrm{d}y_{b,n} \\ \mathrm{d}x_{b,n+1} \\ \mathrm{d}y_{b,n+1} \end{bmatrix} + \mathbf{M}_\mathrm{C} \cdot \mathrm{d}c + \mathbf{M}_\mathrm{H} \cdot \begin{bmatrix} \mathrm{d}z_{0,n} \\ \mathrm{d}z_{i,n} \\ \mathrm{d}z_{0,n+1} \\ \mathrm{d}z_{i,n+1} \end{bmatrix} = 0$$

where, $\mathbf{M}_i$, $\mathbf{M}_\mathrm{T}$, $\mathbf{M}_\mathrm{INS}$, $\mathbf{M}_\mathrm{B}$, $\mathbf{M}_\mathrm{C}$, and $\mathbf{M}_\mathrm{H}$ are the partial differential matrixes. We have

$$\mathbf{M}_i = \begin{bmatrix} \frac{\partial q_1}{\partial x_{0,n}} & \frac{\partial q_1}{\partial y_{0,n}} & \frac{\partial q_1}{\partial x_{i,n}} & \frac{\partial q_1}{\partial y_{i,n}} \\ \frac{\partial q_2}{\partial x_{0,n}} & \frac{\partial q_2}{\partial y_{0,n}} & \frac{\partial q_2}{\partial x_{i,n}} & \frac{\partial q_2}{\partial y_{i,n}} \\ \frac{\partial q_3}{\partial x_{0,n}} & \frac{\partial q_3}{\partial y_{0,n}} & \frac{\partial q_3}{\partial x_{i,n}} & \frac{\partial q_3}{\partial y_{i,n}} \\ \frac{\partial q_4}{\partial x_{0,n}} & \frac{\partial q_4}{\partial y_{0,n}} & \frac{\partial q_4}{\partial x_{i,n}} & \frac{\partial q_4}{\partial y_{i,n}} \end{bmatrix}$$

$$\mathbf{M}_{\mathrm{T}} = \begin{bmatrix} \frac{\partial q_1}{\partial d_{bi,n}} & \frac{\partial q_1}{\partial d_{mi,n}} & \frac{\partial q_1}{\partial d_{bi,n+1}} & \frac{\partial q_1}{\partial d_{mi,n+1}} \\ \frac{\partial q_2}{\partial d_{bi,n}} & \frac{\partial q_2}{\partial d_{mi,n}} & \frac{\partial q_2}{\partial d_{bi,n+1}} & \frac{\partial q_2}{\partial d_{mi,n+1}} \\ \frac{\partial q_3}{\partial d_{bi,n}} & \frac{\partial q_3}{\partial d_{mi,n}} & \frac{\partial q_3}{\partial d_{bi,n+1}} & \frac{\partial q_3}{\partial d_{mi,n+1}} \\ \frac{\partial q_4}{\partial d_{bi,n}} & \frac{\partial q_4}{\partial d_{mi,n}} & \frac{\partial q_4}{\partial d_{bi,n+1}} & \frac{\partial q_4}{\partial d_{mi,n+1}} \end{bmatrix}$$

$$\mathbf{M}_{\mathrm{INS}} = \begin{bmatrix} \frac{\partial q_1}{\partial \Delta x_{0,n}} & \frac{\partial q_1}{\partial \Delta y_{0,n}} & \frac{\partial q_1}{\partial \Delta x_{i,n}} & \frac{\partial q_1}{\partial \Delta y_{i,n}} \\ \frac{\partial q_2}{\partial \Delta x_{0,n}} & \frac{\partial q_2}{\partial \Delta y_{0,n}} & \frac{\partial q_2}{\partial \Delta x_{i,n}} & \frac{\partial q_2}{\partial \Delta y_{i,n}} \\ \frac{\partial q_3}{\partial \Delta x_{0,n}} & \frac{\partial q_3}{\partial \Delta y_{0,n}} & \frac{\partial q_3}{\partial \Delta x_{i,n}} & \frac{\partial q_3}{\partial \Delta y_{i,n}} \\ \frac{\partial q_4}{\partial \Delta x_{0,n}} & \frac{\partial q_4}{\partial \Delta y_{0,n}} & \frac{\partial q_4}{\partial \Delta x_{i,n}} & \frac{\partial q_4}{\partial \Delta y_{i,n}} \end{bmatrix}$$

$$\mathbf{M}_{\mathrm{B}} = \begin{bmatrix} \frac{\partial q_1}{\partial x_{b,n}} & \frac{\partial q_1}{\partial y_{b,n}} & \frac{\partial q_1}{\partial x_{b,n+1}} & \frac{\partial q_1}{\partial y_{b,n+1}} \\ \frac{\partial q_2}{\partial x_{b,n}} & \frac{\partial q_2}{\partial y_{b,n}} & \frac{\partial q_2}{\partial x_{b,n+1}} & \frac{\partial q_2}{\partial y_{b,n+1}} \\ \frac{\partial q_3}{\partial x_{b,n}} & \frac{\partial q_3}{\partial y_{b,n}} & \frac{\partial q_3}{\partial x_{b,n+1}} & \frac{\partial q_3}{\partial y_{b,n+1}} \\ \frac{\partial q_4}{\partial x_{b,n}} & \frac{\partial q_4}{\partial y_{b,n}} & \frac{\partial q_4}{\partial x_{b,n+1}} & \frac{\partial q_4}{\partial y_{b,n+1}} \end{bmatrix}$$

$$\mathbf{M}_{\mathrm{Z}} = \begin{bmatrix} \frac{\partial q_1}{\partial z_{0,n}} & \frac{\partial q_1}{\partial z_{0,n+1}} & \frac{\partial q_1}{\partial z_{i,n}} & \frac{\partial q_1}{\partial z_{i,n+1}} \\ \frac{\partial q_2}{\partial z_{0,n}} & \frac{\partial q_2}{\partial z_{0,n+1}} & \frac{\partial q_2}{\partial z_{i,n}} & \frac{\partial q_2}{\partial z_{i,n+1}} \\ \frac{\partial q_3}{\partial z_{0,n}} & \frac{\partial q_3}{\partial z_{0,n+1}} & \frac{\partial q_3}{\partial z_{i,n}} & \frac{\partial q_3}{\partial z_{i,n+1}} \\ \frac{\partial q_4}{\partial z_{0,n}} & \frac{\partial q_4}{\partial z_{0,n+1}} & \frac{\partial q_4}{\partial z_{i,n}} & \frac{\partial q_4}{\partial z_{i,n+1}} \end{bmatrix},$$

$$\mathbf{M}_{\mathrm{C}} = \begin{bmatrix} \frac{\partial q_1}{\partial c} \\ \frac{\partial q_2}{\partial c} \\ \frac{\partial q_3}{\partial c} \\ \frac{\partial q_4}{\partial c} \end{bmatrix}$$

where,

$$\begin{aligned} q_1 &= \sqrt{(\mathbf{X}_{i,n} - \mathbf{X}_{b,n}) \cdot (\mathbf{X}_{i,n} - \mathbf{X}_{b,n})^{\mathrm{T}}} \\ &\quad + \sqrt{(\mathbf{X}_{0,n} - \mathbf{X}_{b,n}) \cdot (\mathbf{X}_{0,n} - \mathbf{X}_{b,n})^{\mathrm{T}}} - cd_{bi,n} \\ q_2 &= \sqrt{(\mathbf{X}_{i,n} - \mathbf{X}_{0,n}) \cdot (\mathbf{X}_{i,n} - \mathbf{X}_{0,n})^{\mathrm{T}}} - cd_{mi,n} \\ q_3 &= \sqrt{(\mathbf{X}_{i,n+1} - \mathbf{X}_{b,n+1}) \cdot (\mathbf{X}_{i,n+1} - \mathbf{X}_{b,n+1})^{\mathrm{T}}} \\ &\quad + \sqrt{(\mathbf{X}_{0,n+1} - \mathbf{X}_{b,n+1}) \cdot (\mathbf{X}_{0,n+1} - \mathbf{X}_{b,n+1})^{\mathrm{T}}} \\ &\quad - cd_{bi,n+1} \\ q_4 &= \sqrt{(\mathbf{X}_{i,n+1} - \mathbf{X}_{0,n+1}) \cdot (\mathbf{X}_{i,n+1} - \mathbf{X}_{0,n+1})^{\mathrm{T}}} - cd_{mi,n+1} \end{aligned}$$

Transforming the partial differential equation, we have

$$\begin{aligned} \begin{bmatrix} \mathrm{d}x_{0,n} \\ \mathrm{d}y_{0,n} \\ \mathrm{d}x_{i,n} \\ \mathrm{d}y_{i,n} \end{bmatrix} &= -\mathbf{M}_i^{-1} \cdot \{\mathbf{M}_{\mathrm{T}} \cdot \begin{bmatrix} \mathrm{d}d_{bi,n} \\ \mathrm{d}d_{mi,n} \\ \mathrm{d}d_{bi,n+1} \\ \mathrm{d}d_{mi,n+1} \end{bmatrix} \\ &\quad + \mathbf{M}_{\mathrm{INS}} \cdot \begin{bmatrix} \mathrm{d}\Delta x_{0,n} \\ \mathrm{d}\Delta y_{0,n} \\ \mathrm{d}\Delta x_{i,n} \\ \mathrm{d}\Delta y_{i,n} \end{bmatrix} + \mathbf{M}_{\mathrm{B}} \cdot \begin{bmatrix} \mathrm{d}x_{b,n} \\ \mathrm{d}y_{b,n} \\ \mathrm{d}x_{b,n+1} \\ \mathrm{d}y_{b,n+1} \end{bmatrix} \\ &\quad + \mathbf{M}_{\mathrm{C}} \cdot \mathrm{d}c + \mathbf{M}_{\mathrm{H}} \cdot \begin{bmatrix} \mathrm{d}z_{0,n} \\ \mathrm{d}z_{i,n} \\ \mathrm{d}z_{0,n+1} \\ \mathrm{d}z_{i,n+1} \end{bmatrix} \} \end{aligned}$$

Then, the covariance matrix of AUV's coordinate can be obtained as

$$\begin{aligned} \mathbf{D}_i &= E(\begin{bmatrix} \mathrm{d}x_{0,n} \\ \mathrm{d}y_{0,n} \\ \mathrm{d}x_{i,n} \\ \mathrm{d}y_{i,n} \end{bmatrix} \cdot \begin{bmatrix} \mathrm{d}x_{0,n} \\ \mathrm{d}y_{0,n} \\ \mathrm{d}x_{i,n} \\ \mathrm{d}y_{i,n} \end{bmatrix}^{\mathrm{T}}) \\ &= \mathbf{M}_i^{-1} \cdot \{\mathbf{M}_{\mathrm{T}} \cdot (\begin{bmatrix} \mathrm{d}d_{bi,n} \\ \mathrm{d}d_{mi,n} \\ \mathrm{d}d_{bi,n+1} \\ \mathrm{d}d_{mi,n+1} \end{bmatrix} \cdot \begin{bmatrix} \mathrm{d}d_{bi,n} \\ \mathrm{d}d_{mi,n} \\ \mathrm{d}d_{bi,n+1} \\ \mathrm{d}d_{mi,n+1} \end{bmatrix}^{\mathrm{T}}) \cdot \mathbf{M}_{\mathrm{T}}^{\mathrm{T}} \\ &\quad + \mathbf{M}_{\mathrm{INS}} \cdot (\begin{bmatrix} \mathrm{d}\Delta x_{0,n} \\ \mathrm{d}\Delta y_{0,n} \\ \mathrm{d}\Delta x_{i,n} \\ \mathrm{d}\Delta y_{i,n} \end{bmatrix} \cdot \begin{bmatrix} \mathrm{d}\Delta x_{0,n} \\ \mathrm{d}\Delta y_{0,n} \\ \mathrm{d}\Delta x_{i,n} \\ \mathrm{d}\Delta y_{i,n} \end{bmatrix}^{\mathrm{T}}) \cdot \mathbf{M}_{\mathrm{INS}}^{\mathrm{T}} \\ &\quad + \mathbf{M}_{\mathrm{B}} \cdot (\begin{bmatrix} \mathrm{d}x_{b,n} \\ \mathrm{d}y_{b,n} \\ \mathrm{d}x_{b,n+1} \\ \mathrm{d}y_{b,n+1} \end{bmatrix} \cdot \begin{bmatrix} \mathrm{d}x_{b,n} \\ \mathrm{d}y_{b,n} \\ \mathrm{d}x_{b,n+1} \\ \mathrm{d}y_{b,n+1} \end{bmatrix}^{\mathrm{T}}) \cdot \mathbf{M}_{\mathrm{B}}^{\mathrm{T}} \\ &\quad + \mathbf{M}_{\mathrm{H}} \cdot (\begin{bmatrix} \mathrm{d}z_{0,n} \\ \mathrm{d}z_{i,n} \\ \mathrm{d}z_{0,n+1} \\ \mathrm{d}z_{i,n+1} \end{bmatrix} \cdot \begin{bmatrix} \mathrm{d}z_{0,n} \\ \mathrm{d}z_{i,n} \\ \mathrm{d}z_{0,n+1} \\ \mathrm{d}z_{i,n+1} \end{bmatrix}^{\mathrm{T}}) \cdot \mathbf{M}_{\mathrm{H}}^{\mathrm{T}} \\ &\quad + \mathbf{M}_{\mathrm{C}} \cdot \mathrm{d}c\mathrm{d}c \cdot \mathbf{M}_{\mathrm{C}}^{\mathrm{T}}\} \cdot \mathbf{M}_i^{-1\mathrm{T}} \\ &= \mathbf{M}_i^{-1} \cdot \{\mathbf{M}_{\mathrm{T}} \cdot \mathbf{D}_{\mathrm{T}} \cdot \mathbf{M}_{\mathrm{T}}^{\mathrm{T}} + \mathbf{M}_{\mathrm{INS}} \cdot \mathbf{D}_{\mathrm{INS}} \cdot \mathbf{M}_{\mathrm{INS}}^{\mathrm{T}} \\ &\quad + \mathbf{M}_{\mathrm{B}} \cdot \mathbf{D}_{\mathrm{B}} \cdot \mathbf{M}_{\mathrm{B}}^{\mathrm{T}} + \mathbf{M}_{\mathrm{C}} \cdot \mathbf{D}_{\mathrm{C}} \cdot \mathbf{M}_{\mathrm{C}}^{\mathrm{T}} \\ &\quad + \mathbf{M}_{\mathrm{H}} \cdot \mathbf{D}_{\mathrm{H}} \cdot \mathbf{M}_{\mathrm{H}}^{\mathrm{T}}\} \cdot \mathbf{M}_i^{-1\mathrm{T}} \end{aligned}$$

where, $\mathbf{D}_{\mathrm{T}}$, $\mathbf{D}_{\mathrm{INS}}$, $\mathbf{D}_{\mathrm{B}}$, $\mathbf{D}_{\mathrm{C}}$, and $\mathbf{D}_{\mathrm{H}}$ are the covariance matrixes, $\mathbf{D}_{\mathrm{T}} = \mathrm{diag}([\sigma^2_{d_{bi,n}}, \sigma^2_{d_{mi,n}}, \sigma^2_{d_{bi,n+1}}, \sigma^2_{d_{mi,n+1}}])$, $\mathbf{D}_{\mathrm{INS}} = \mathrm{diag}([\sigma^2_{\Delta x_{0,n}}, \sigma^2_{\Delta y_{0,n}}, \sigma^2_{\Delta x_{i,n}}, \sigma^2_{\Delta y_{i,n}}])$, $\mathbf{D}_{\mathrm{B}} = \mathrm{diag}([\sigma^2_{x_{b,n}}, \sigma^2_{y_{b,n}}, \sigma^2_{x_{b,n+1}}, \sigma^2_{y_{b,n+1}}])$, $\mathbf{D}_{\mathrm{C}} = \sigma_c^2$, $\mathbf{D}_{\mathrm{H}} = \mathrm{diag}([\sigma^2_{z_{0,n}}, \sigma^2_{z_{i,n}}, \sigma^2_{z_{0,n+1}}, \sigma^2_{z_{i,n+1}}])$. $\mathrm{diag}(*)$ indicates the diagonal matrix, and σ_*^2 means the variance.

APPENDIX B
DETAILED EXPRESSION OF (11)

$$\begin{aligned} \hat{\mathbf{X}} = [&v_0 \cos\varphi_0 cos\theta_0 \Delta t, v_0 \sin\varphi_0 cos\theta_0 \Delta t, \\ &v_i cos\varphi_i cos\theta_i \Delta t, v_i \sin\varphi_i cos\theta_i \Delta t]^T \end{aligned}$$

$$f_1 = \frac{\partial \hat{\mathbf{X}}}{\partial v_0} = [\cos\varphi_0 cos\theta_0 \Delta t, \sin\varphi_0 cos\theta_0 \Delta t, 0, 0]^T$$

$$f_2 = \frac{\partial \hat{\mathbf{X}}}{\partial \varphi_0} = [-v_0 \sin\varphi_0 cos\theta_0 \Delta t, v_0 \cos\varphi_0 cos\theta_0 \Delta t, 0, 0]^T$$

$$f_3 = \frac{\partial \hat{\mathbf{X}}}{\partial \theta_0} = [-v_0 \cos\varphi_0 \sin\theta_0 \Delta t, -v_0 \sin\varphi_0 \sin\theta_0 \Delta t, 0, 0]^T$$

$$f_4 = \frac{\partial \hat{\mathbf{X}}}{\partial v_i} = [0, 0, \cos\varphi_i cos\theta_i \Delta t, \sin\varphi_i cos\theta_i \Delta t]^T$$

$$f_5 = \frac{\partial \hat{\mathbf{X}}}{\partial \varphi_i} = [0, 0, -v_i \sin\varphi_i cos\theta_i \Delta t, v_i \cos\varphi_i cos\theta_i \Delta t]^T$$

$$f_6 = \frac{\partial \hat{\mathbf{X}}}{\partial \theta_i} = [0, 0, -v_i \cos\varphi_i \sin\theta_i \Delta t, -v_i \sin\varphi_i \sin\theta_i \Delta t]^T$$

We denote $r_{i,k}$ as the distance between two points. (For example, $r_{0,b}$ means the distance between A_0 and B), then we have

$$\nabla L^0 h_0 = \frac{\partial h_0}{\partial \mathbf{X}} = [\frac{x_0 - x_b}{r_{0,b}}, \frac{y_0 - y_b}{r_{0,b}}, \frac{x_i - x_b}{r_{i,b}}, \frac{y_i - y_b}{r_{i,b}}]^T$$

$$L_{f_1}^1 h_0 = \nabla L^0 h_0 \cdot f_1 = \frac{cos\theta_0 \Delta t}{r_{0,b}} \times [(x_0 - x_b)\cos\varphi_0 + (y_0 - y_b)\sin\varphi_0]$$

$$\nabla L_{f_1}^1 h_0 = \frac{\partial L_{f_1}^1 h_0}{\partial \mathbf{X}} = \frac{cos\theta_0 \Delta t}{r_{0,b}}[u_1, u_2, 0, 0]^T$$

$$L_{f_2}^1 h_0 = \nabla L^0 h_0 \cdot f_2 = \frac{v_0 cos\theta_0 \Delta t}{r_{0,b}} \times [(y_0 - y_b)\cos\varphi_0 - (x_0 - x_b)\sin\varphi_0]$$

$$\nabla L_{f_2}^1 h_0 = \frac{\partial L_{f_2}^1 h_0}{\partial \mathbf{X}} = \frac{v_0 cos\theta_0 \Delta t}{r_{0,b}}[u_3, u_4, 0, 0]^T$$

$$L_{f_3}^1 h_0 = \nabla L^0 h_0 \cdot f_3 = -\frac{v_0 \sin\theta_0 \Delta t}{r_{0,b}} \times [(x_0 - x_b)\cos\varphi_0 + (y_0 - y_b)\sin\varphi_0]$$

$$\nabla L_{f_3}^1 h_0 = \frac{\partial L_{f_3}^1 h_0}{\partial \mathbf{X}} = -\frac{v_0 \sin\theta_0 \Delta t}{r_{0,b}}[u_1, u_2, 0, 0]^T$$

$$L_{f_4}^1 h_0 = \nabla L^0 h_0 \cdot f_4 = \frac{cos\theta_i \Delta t}{r_{i,b}} \times [(x_i - x_b)\cos\varphi_i + (y_i - y_b)\sin\varphi_i]$$

$$\nabla L_{f_4}^1 h_0 = \frac{\partial L_{f_4}^1 h_0}{\partial \mathbf{X}} = \frac{cos\theta_i \Delta t}{r_{i,b}}[0, 0, u_5, u_6]^T$$

$$L_{f_5}^1 h_0 = \nabla L^0 h_0 \cdot f_5 = \frac{v_i cos\theta_i \Delta t}{r_{i,b}} \times [(y_i - y_b)\cos\varphi_i - (x_i - x_b)\sin\varphi_i]$$

$$\nabla L_{f_5}^1 h_0 = \frac{\partial L_{f_5}^1 h_0}{\partial \mathbf{X}} = \frac{v_i cos\theta_i \Delta t}{r_{i,b}}[0, 0, u_7, u_8]^T$$

$$L_{f_6}^1 h_0 = \nabla L^0 h_0 \cdot f_6 = -\frac{v_i \sin\theta_i \Delta t}{r_{i,b}} \times [(x_i - x_b)\cos\varphi_i + (y_i - y_b)\sin\varphi_i]$$

$$\nabla L_{f_6}^1 h_0 = \frac{\partial L_{f_6}^1 h_0}{\partial \mathbf{X}} = -\frac{v_i \sin\theta_i \Delta t}{r_{i,b}}[0, 0, u_5, u_6]^T$$

$$\nabla L^0 h_1 = \frac{\partial h_1}{\partial \mathbf{X}} = [\frac{x_0 - x_i}{r_{0,i}}, \frac{y_0 - y_i}{r_{0,i}}, \frac{x_i - x_0}{r_{0,i}}, \frac{y_i - y_0}{r_{0,i}}]^T$$

$$L_{f_1}^1 h_1 = \nabla L^0 h_1 \cdot f_1 = \frac{cos\theta_0 \Delta t}{r_{0,i}} \times [(x_0 - x_i)\cos\varphi_0 + (y_0 - y_i)\sin\varphi_0]$$

$$\nabla L_{f_1}^1 h_1 = \frac{\partial L_{f_1}^1 h_1}{\partial \mathbf{X}} = \frac{cos\theta_0 \Delta t}{r_{0,i}}[u_9, u_{10}, 0, 0]^T$$

$$L_{f_2}^1 h_1 = \nabla L^0 h_1 \cdot f_2 = \frac{v_0 cos\theta_0 \Delta t}{r_{0,i}} \times [(y_0 - y_i)\cos\varphi_0 - (x_0 - x_i)\sin\varphi_0]$$

$$\nabla L_{f_2}^1 h_1 = \frac{\partial L_{f_2}^1 h_1}{\partial \mathbf{X}} = \frac{v_0 cos\theta_0 \Delta t}{r_{0,i}}[u_{11}, u_{12}, 0, 0]^T$$

$$L_{f_3}^1 h_1 = \nabla L^0 h_1 \cdot f_3 = -\frac{v_0 \sin\theta_0 \Delta t}{r_{0,i}} \times [(x_0 - x_i)\cos\varphi_0 + (y_0 - y_i)\sin\varphi_0]$$

$$\nabla L_{f_3}^1 h_1 = \frac{\partial L_{f_3}^1 h_1}{\partial \mathbf{X}} = -\frac{v_0 \sin\theta_0 \Delta t}{r_{0,i}}[u_9, u_{10}, 0, 0]^T$$

$$L_{f_4}^1 h_1 = \nabla L^0 h_1 \cdot f_4 = \frac{cos\theta_i \Delta t}{r_{0,i}} \times [(x_i - x_0)\cos\varphi_i + (y_i - y_0)\sin\varphi_i]$$

$$\nabla L_{f_4}^1 h_1 = \frac{\partial L_{f_4}^1 h_1}{\partial \mathbf{X}} = \frac{cos\theta_i \Delta t}{r_{0,i}}[0, 0, u_{13}, u_{14}]^T$$

$$L_{f_5}^1 h_1 = \nabla L^0 h_1 \cdot f_5 = \frac{v_i cos\theta_i \Delta t}{r_{0,i}} \times [(y_i - y_0)\cos\varphi_i - (x_i - x_0)\sin\varphi_i]$$

$$\nabla L_{f_5}^1 h_1 = \frac{\partial L_{f_5}^1 h_1}{\partial \mathbf{X}} = \frac{v_i cos\theta_i \Delta t}{r_{0,i}}[0, 0, u_{15}, u_{16}]^T$$

$$L_{f_6}^1 h_1 = \nabla L^0 h_1 \cdot f_6 = -\frac{v_i \sin\theta_i \Delta t}{r_{0,i}} \times [(x_i - x_0)\cos\varphi_i + (y_i - y_0)\sin\varphi_i]$$

$$\nabla L_{f_6}^1 h_1 = \frac{\partial L_{f_6}^1 h_1}{\partial \mathbf{X}} = -\frac{v_i \sin\theta_i \Delta t}{r_{0,i}}[0, 0, u_{13}, u_{14}]^T$$

where, $u_1, u_2, \ldots, u_{16}$ are expressions related to the AUV's motion parameters and it is easily to prove that these atoms are non-zero unless $v_0 = v_i = 0$.

REFERENCES

[1] L. Paull, S. Saeedi, M. Seto, and H. Li, "AUV navigation and localization: A review," *IEEE J. Ocean. Eng.*, vol. 39, no. 1, pp. 131–149, Jan. 2014, doi: 10.1109/JOE.2013.2278891.

[2] F. A. X. Da Nota, M. X. Rocha, J. J. P. C. Rodrigues, V. De Albuquerque, and A. R. De Alexandria, "Localization and navigation for autonomous mobile robots using petri nets in indoor environments," *IEEE Access*, vol. 6, pp. 31665–31676, 2018, doi: 10.1109/ACCESS.2018.2846554.

[3] H. P. Tan, R. Diamant, W. K. G. Seah, and M. Waldmeyer, "A survey of techniques and challenges in underwater localization," *Ocean Eng.*, vol. 38, nos. 14–15, pp. 1663–1676, Oct. 2011, doi: 10.1016/j.oceaneng.2011.07.017.

[4] Y. Tao, L. L. Ding, and A. Ganz, "Indoor navigation validation framework for visually impaired users," *IEEE Access*, vol. 5, pp. 21763–21773, 2017, doi: 10.1109/ACCESS.2017.2761698.

[5] L. Zhao, S. E. Dosso, and D. Sun, "Motion-compensated acoustic localization for underwater vehicles," *IEEE J. Ocean. Eng.*, vol. 41, no. 4, pp. 840–851, Oct. 2016, doi: 10.1109/JOE.2015.2503518.

[6] A. Caiti, A. Garulli, F. Livide, and D. Prattichizzo, "Localization of autonomous underwater vehicles by floating acoustic buoys: A set-membership approach," *IEEE J. Ocean. Eng.*, vol. 30, no. 1, pp. 140–152, Jan. 2005, doi: 10.1109/JOE.2004.841432.

[7] D. Moreno-Salinas, A. Pascoal, and J. Aranda, "Optimal sensor placement for acoustic underwater target positioning with range-only measurements," *IEEE J. Ocean. Eng.*, vol. 41, no. 3, pp. 620–643, Jul. 2016, doi: 10.1109/JOE.2015.2494918.
[8] J. Liu, Z.-H. Wang, J.-H. Cui, S. Zhou, and B. Yang, "A joint time synchronization and localization design for mobile underwater sensor networks," *IEEE Trans. Mobile Comput.*, vol. 15, no. 3, pp. 530–543, Mar. 2016, doi: 10.1109/TMC.2015.2410777.
[9] E. Yuan, W. Qi, P. Liu, L. Wei, and L. Chen, "Ranging method for navigation based on high-speed frequency-hopping signal," *IEEE Access*, vol. 6, pp. 4308–4320, 2018, doi: 10.1109/ACCESS.2017.2787801.
[10] N. H. Kussat, C. D. Chadwell, and R. Zimmerman, "Absolute positioning of an autonomous underwater vehicle using GPS and acoustic measurements," *IEEE J. Ocean. Eng.*, vol. 30, no. 1, pp. 153–164, Jan. 2005, doi: 10.1109/JOE.2004.835249.
[11] Y. T. Tan, R. Gao, and M. Chitre, "Cooperative path planning for range-only localization using a single moving beacon," *IEEE J. Ocean. Eng.*, vol. 39, no. 2, pp. 371–385, Apr. 2014, doi: 10.1109/JOE.2013.2296361.
[12] T. Maki, T. Matsuda, T. Sakamaki, T. Ura, and J. Kojima, "Navigation method for underwater vehicles based on mutual acoustical positioning with a single seafloor station," *IEEE J. Ocean. Eng.*, vol. 38, no. 1, pp. 167–177, Jan. 2013, doi: 10.1109/JOE.2012.2210799.
[13] A. Gatsenko, F. Dubrovin, and A. Scherbatyuk, "Comparing some algorithms for AUV single beacon mobile navigation," in *Proc. Oceans Conf.*, Sep. 2014, pp. 1–5, doi: 10.1109/OCEANS.2014.7003048.
[14] H. Wang, L. Wu, H. Chai, H. Hsu, and Y. Wang, "Technology of gravity aided inertial navigation system and its trial in South China Sea," *IET Radar Sonar and Navigat.*, vol. 10, no. 5, pp. 862–869, Jun. 2016, doi: 10.1049/iet-rsn.2014.0419.
[15] S. E. Webster, R. M. Eustice, H. Singh, and L. L. Whitcomb, "Advances in single-beacon one-way-travel-time acoustic navigation for underwater vehicles," *Int. J. Robot. Res.*, vol. 31, no. 8, pp. 935–950, 2012, doi: 10.1177/0278364912446166.
[16] H. Yang, W. Li, C. Luo, J. Zhang, and Z. Si, "Research on error compensation property of strapdown inertial navigation system using dynamic model of shearer," *IEEE Access*, vol. 4, pp. 2045–2055, 2016, doi: 10.1109/ACCESS.2016.2565638.
[17] J. M. Kelner, C. Ziółkowski, L. Nowosielski, and M. Wnuk, "Reserve navigation system for ships based on coastal radio beacons," in *Proc. IEEE/ION Position, Location, Navigat. Symp.*, Apr. 2016, pp. 393–402, doi: 10.1109/PLANS.2016.7479726.
[18] W. Xu, F. Sun, and J. Li, "Integrated navigation for an autonomous underwater vehicle carrying synthetic aperture sonar," *IET Radar, Sonar Navigat.*, vol. 6, no. 9, pp. 905–912, Dec. 2012, doi: 10.1049/iet-rsn.2011.0291.
[19] J. Bosch, N. Gracias, P. Ridao, K. Istenič, and D. Ribas, "Close-range tracking of underwater vehicles using light beacons," *Sensors*, vol. 16, no. 4, p. 429, Apr. 2016, doi: 10.3390/s16040429.
[20] A. A. Lunkov, V. G. Petnikov, and A. D. Chernousov, "Estimating the effective sound speed in the bottom in shallow water areas," *Acoust. Phys.*, vol. 61, no. 6, pp. 707–714, Apr. 2015, doi: 10.1134/S1063771015060081.
[21] Y. Yang, C. Zhang, J. Lu, and H. Zhang, "Classification of methods in the SINS/CNS integration navigation system," *IEEE Access*, vol. 6, pp. 3149–3158, 2018, doi: 10.1109/ACCESS.2017.2787424.
[22] H. Huang *et al.*, "Attitude estimation fusing Quasi-Newton and cubature Kalman filtering for inertial navigation system aided with magnetic sensors," *IEEE Access*, vol. 6, pp. 28755–28767, 2018, doi: 10.1109/ACCESS.2018.2833290.
[23] K. H. Tang, J. Wang, W. Li, and W. Wu, "A novel INS and Doppler sensors calibration method for long range underwater vehicle navigation," *Sensors*, vol. 13, no. 11, pp. 14583–14600, 2013, doi: 10.3390/s131114583.
[24] C. Liu, P. Shui, and S. Li, "Unscented extended Kalman filter for target tracking," *J. Syst. Eng. Electron.*, vol. 22, no. 2, pp. 188–192, Apr. 2011, doi: 10.3969/j.issn.1004-4132.2011.02.002.
[25] H. Wang, J. Wang, X. Bian, and G. Fu, "SLAM of AUV based on the combined EKF," *Robot*, vol. 22, no. 5, pp. 728–740, 1977, doi: 10.3724/SPJ.1218.2012.00056.
[26] A. J. Whalen, S. N. Brennan, T. D. Sauer, and S. J. Schiff, "Observability and controllability of nonlinear networks: The role of symmetry," *Phys. Rev. X*, vol. 5, no. 1, p. 011005, Jan. 2015, doi: 10.1103/PhysRevX.5.011005.
[27] A. S. Gadre and D. J. Stilwell, "Underwater navigation in the presence of unknown currents based on range measurements from a single location," in *Proc. Amer. Control Conf.*, Jun. 2015, pp. 656–661, doi: 10.1109/ACC.2005.1470032.
[28] I. Arasaratnam and S. Haykin, "Cubature Kalman filters," *IEEE Trans. Autom. Control*, vol. 54, no. 6, pp. 1254–1269, Jun. 2009, doi: 10.1109/TAC.2009.2019800.
[29] M. S. Arulampalam, S. Maskell, N. Gordon, and T. Clapp, "A tutorial on particle filters for online nonlinear/non-Gaussian Bayesian tracking," *IEEE Trans. Signal Process.*, vol. 50, no. 2, pp. 174–188, Feb. 2002, doi: 10.1109/78.978374.

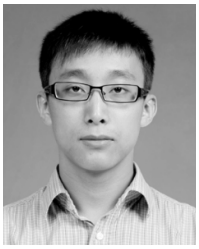

SIBO SUN was born in Harbin, China, in 1987. He received the B.E. and Ph.D. degrees from the Harbin Institute of Technology in 2010 and 2017, respectively. He studied in the National University of Singapore in 2014. He is currently an Associate Professor with Harbin Engineering University. His research interests include radar imaging, sonar imaging, and positioning.

SHUANGNING YU was born in Weifang, China, in 1995. He received the B.E. degree from the Harbin Institute of Technology in 2017. He is currently pursuing the master's degree with Harbin Engineering University. His research interests include sonar positioning.

ZHIBO SHI was born in Henan, China, in 1990. He received the B.E. degree from Harbin Engineering University, Harbin, China, in 2013, where he is currently pursuing the Ph.D. degree with the College of Underwater Acoustic Engineering. His research interests include array signal processing, sparse signal representation, and positioning.

JIN FU was born in 1981. He is currently a Professor with the College of Underwater Acoustic Engineering, Harbin Engineering University. He is currently researching on sonar localization and sonar detection.

CHUNHUI ZHAO received the Ph.D. degree from the Harbin Institute of Technology in 1998. He is currently a Professor with the College of Information and Communication Engineering, Harbin Engineering University. His current research interests are in sonar signal processing, image processing, and hyperspectral imaging.